Resonant Raman scattering of single molecules under simultaneous strong cavity coupling and ultrastrong optomechanical coupling in plasmonic resonators: Phonon-dressed polaritons

Stephen Hughes [1], Alessio Settineri,[2] Salvatore Savasta,[2] and Franco Nori [3,4]

[1]*Department of Physics, Engineering Physics and Astronomy, Queen's University, Kingston, Ontario, Canada K7L 3N6*
[2]*Dipartimento di Scienze Matematiche e Informatiche, Scienze Fisiche e Scienze della Terra, Università di Messina, I-98166 Messina, Italy*
[3]*Theoretical Quantum Physics Laboratory, RIKEN Cluster for Pioneering Research, Wako-shi, Saitama 351-0198, Japan*
[4]*Physics Department, The University of Michigan, Ann Arbor, Michigan 48109-1040, USA*

Plasmonic dimer cavities can induce extreme electric-field hot spots that allow one to access ultrastrong coupling regimes using Raman-type spectroscopy on single vibrating molecules. Using a generalized master equation, we study resonant Raman scattering in the strong coupling regime of cavity quantum electrodynamics, when also in the vibrational ultrastrong coupling regime, leading to "phonon-dressed polaritons." The master equation rigorously includes spectral baths for the cavity and vibrational degrees of freedom, as well as a pure dephasing bath for the resonant two-level system, which play a significant role. Employing realistic parameters for gold dimer cavity modes, we investigate the emission spectra in several characteristic strong coupling regimes, leading to extremely rich spectral resonances due to an interplay of phonon-modified polariton states and bath-induced resonances. We also show explicitly the failure of the standard master equation in these quantum nonlinear regimes.

I. INTRODUCTION

The celebrated Raman effect is based on the inelastic scattering of monochromatic incident radiation, whereby coherent optical fields couple to molecular vibrations and scatter at phonon-shifted frequencies with respect to the excitation frequency [1]. The usual Raman interaction leads to Stokes emission (lower energies) and anti-Stokes emission (higher energies). Although most Raman experiments deal with very weak scattering cross sections, surface-enhanced Raman spectroscopy (SERS) with metal nanoparticles (MNPs) can boost this interaction by many orders of magnitude.

While there is much interest in using MNPs to explore new regimes in quantum plasmonics [2–12], a major problem for enhancing quantum light-matter interactions is metallic losses. In contrast to dielectric cavity systems, the quality factors for MNPs are only around $Q \sim 5$–20, resulting in significant cavity decay rates κ, typically too large to resolve higher-lying quantum states. However, plasmonic resonator cavity modes also yield extremely small mode volumes that can compensate for the large losses. Thus treating the plasmonic system as a "bath" is not necessarily a good approximation, and quantum correlations can be important.

In the field of optomechanics, photon-photon interactions with vibrational interactions can give rise to interesting correlation effects [13], but accessing such regimes has proven experimentally difficult, and often the problem is treated through various linearization procedures, where the photons are not entangled with the phonons. Recently, it has also been shown how SERS can be viewed as an effective enhancement of the optomechanical coupling between the localized surface plasmon resonance and the vibrational mode of the molecule, leading to new ideas in *molecular optomechanics* [14–16]. In such regimes, the plasmon mode and vibrating molecule mimic the optomechanical coupling scenario with a one-dimensional (1D) cavity mode in the presence of a vibrating mirror [14]. Potential advantages of molecular optomechanics, over dielectric-based systems, include access to higher vibrational frequencies and larger optomechanical coupling rates. Several key experiments in this area have emerged, including pulsed molecular optomechanics [17]. For hybrid metal-dielectric resonances, molecular optomechanics in the sideband-resolved regime has also been predicted [18]. Vibronic strong coupling effects in Raman scattering have also been studied [19], using a quantum theory of strong coupling of collective molecular vibrations [that are infrared (IR) active] within a microcavity.

One way to boost the optomechanical rates even further is to use *resonant* electronic excitations (see Fig. 1), which brings in the traditional domains of cavity quantum electrodynamics (QED), and modified optomechanical coupling with Fermionic statistics. Molecular two-level systems (TLSs) coupled to MNPs have already shown experimental signatures of vacuum Rabi splitting [6], where it is also noted there there are rich Raman transitions involved [6]. To understand such emerging systems, one must couple the physics of resonant SERS and traditional cavity-QED physics, while properly accounting for vibrational ultrastrong coupling (USC) and complex bath interactions, in regimes where traditional master equations can significantly fail.
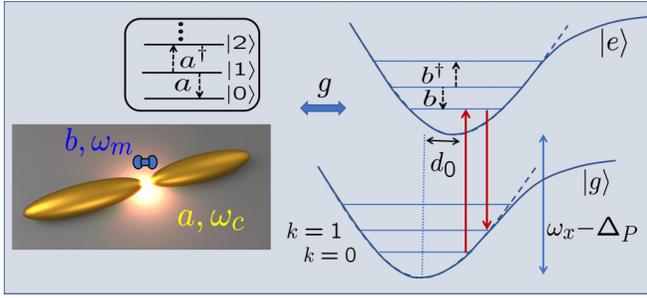
FIG. 1. Schematic of a plasmonic field hot spot coupled to a vibrating molecule $(b, b^\dagger)$ and the cavity mode ladder states $(a, a^\dagger)$. At the right, we also show the two electronic manifolds, each containing a subset of phonon levels $(k = 0, 1, \ldots)$ separated by ω_m and coupled to the cavity mode through g; the excited manifold is shifted down from the bare exciton resonance ω_x through the polaron shift $\Delta_P = d_0^2 \omega_m$ and shifted by the normalized displacement d_0.

Several resonant SERS schemes have been theoretically studied with various limitations. A bad-cavity limit has been used to explore the interplay between TLS driving and vibrational coupling [20], where the Mollow triplet resonances can be split by phonon interactions; the theory employed a standard master equation (SME) with simple TLS pure dephasing processes. Also using a SME, Ref. [21] studied resonant SERS in the good-cavity limit, presenting useful analytical solutions and numerical results of hybrid resonances; however, for vibrational USC, the SME breaks down. Recently, USC in molecular cavity QED using the quantum Rabi model has been explored [22], where model Hamiltonians and dynamical coupling in a one-photon subspace were studied, though dissipation was neglected.

In this paper, we present a theory of MNP-based single molecular optomechanics in the strong cavity-coupled *nonlinear* resonant Raman regime, fully accounting for the dynamics of the system level operators for the TLS, the cavity mode, and a molecular phonon mode. We rigorously treat system-bath dissipation by using a generalized master equation (GME) approach, modeled with characteristic spectral functions for the photon and phonon baths as well as excitonic pure dephasing. We also show explicitly how the SME fails in such regimes. Indeed, the GME is shown to yield much richer spectral features because of bath-induced interactions. We explore several regimes of simultaneous strong cavity-exciton coupling and vibrational coupling in the USC regime [23,24], showing extremely rich cavity emitted spectra, including phonon-dressed strong coupling with resonant Raman scattering. These effects are also influenced by the presence of multiple bath-induced asymmetries and modified resonances.

II. THEORY

To make a connection with off-resonance Raman interactions, it is useful to first consider the standard optomechanical Hamiltonian [25] $(\hbar = 1)$,

$$H_s = \omega_c a^\dagger a + \omega_m b^\dagger b - g_{\text{om}} a^\dagger a(b^\dagger + b), \quad (1)$$

where ω_m is the molecular vibrational mode frequency, ω_c is the cavity mode resonance frequency, and $a, a^\dagger$ and $b, b^\dagger$ are

the annihilation and creation operators for the cavity mode and phonon mode, respectively. The eigenenergies of Eq. (1) are [26]

$$\omega_{n,k} = n\omega_c + k\omega_m - n^2 g_{\text{om}}^2/\omega_m, \quad (2)$$

with the corresponding eigenstates,

$$|\Psi_{n,k}\rangle = D^\dagger(g_{\text{om}}n/\omega_m)|n, k\rangle, \quad (3)$$

where D is the displacement operator. The displacement of phonons also depends on the number of photons. This results in photon manifolds that contain phonon sublevels, and each manifold is shifted down in energy from the cavity resonance. In a polaronic frame, the cavity mode frequency changes from

$$\omega_c \rightarrow \omega_c - g_{\text{om}}^2/\omega_m = \omega_c - d_0^2 \omega_m, \quad (4)$$

where d_0 is a dimensionless displacement [20].

For resonant Raman interactions, we assume that the plasmonic MNP interacts with electronic TLS vibrational degrees of freedom through a Huang-Rhys theory, first formulated for F centers in 1950 [20,27–29], which has been widely used to model vibronic interaction in molecules [19,30] and has the same form as electron-phonon scattering in quantum dot systems [29,31–34]. The system Hamiltonian is

$$H_s = \omega_c a^\dagger a + \omega_x \sigma^+ \sigma^- + \omega_m b^\dagger b + d_0 \omega_m \sigma^+ \sigma^-(b^\dagger + b)$$
$$+ g(\sigma^+ a + a^\dagger \sigma^-), \quad (5)$$

where ω_x is the exciton resonance frequency and the latter term is the Jaynes-Cummings interaction, where we assume $g \ll \omega_c$, and thus neglect USC effects from the cavity-TLS interaction. However, USC effects from vibrational coupling are fully included.

With system-bath interactions included, the SME for resonant SERS with a single MNP cavity mode is [35,36]

$$\frac{d\rho(t)}{dt} = -i[H_s, \rho(t)] + \frac{\kappa}{2}\mathcal{D}[a]\rho(t) + \frac{\gamma_\phi}{2}\mathcal{D}[\sigma^+\sigma^-]\rho(t)$$

$$+ \frac{\gamma_m(\bar{n}_m + 1)}{2}\mathcal{D}[b]\rho(t) + \frac{\gamma_m\bar{n}_m}{2}\mathcal{D}[b^\dagger]\rho(t), \quad (6)$$

where κ is the cavity decay rate (which dominates over spontaneous emission), γ_ϕ is a possible pure dephasing rate of the TLS, γ_m is the vibrational decay rate, and $\bar{n}_m = 1/[\exp(\omega_m/T) - 1]$ is the thermal population of the vibrational mode at temperature T (in units of $k_B = 1$). The system Hamiltonian is given in Eq. (5), and the Lindblad superoperator is defined by

$$\mathcal{D}[O]\rho(t) = O\rho(t)O^\dagger - 0.5O^\dagger O\rho(t) - 0.5\rho(t)O^\dagger O. \quad (7)$$

A known problem with the SME is that it neglects the internal coupling between the system operators when deriving the system-bath interactions [8,37–39]. To address this problem, we exploit a GME approach [39], which takes into account the dressed states' coupling to the bath reservoirs:

$$\frac{d}{dt}\rho = -i[H_s, \rho] + \mathcal{L}_G\rho + \mathcal{L}_G^\phi\rho, \quad (8)$$

where the dissipator term

$$\mathcal{L}_G \rho = \frac{1}{2} \sum_{\alpha=c,m} \sum_{\omega,\omega'>0}$$

$$\Gamma_\alpha(\omega)(1+\bar{n}_\alpha(\omega))[x^+(\omega)\rho x^-(\omega') - x^-(\omega')x^+(\omega)\rho]$$

$$+ \Gamma_\alpha(\omega')(1+\bar{n}_\alpha(\omega'))[x^+(\omega)\rho x^-(\omega') - \rho x^-(\omega')x^+(\omega)]$$

$$+ \Gamma_\alpha(\omega)\bar{n}_\alpha(\omega)[x^-(\omega')\rho x^+(\omega) - \rho x^+(\omega)x^-(\omega')]$$

$$+ \Gamma_\alpha(\omega')\bar{n}_\alpha(\omega')[x^-(\omega')\rho x^+(\omega) - x^+(\omega)x^-(\omega')\rho]$$

$$+ \Gamma'_\alpha(T)[2x^0_\alpha \rho x^0_\alpha - x^0_\alpha x^0_\alpha \rho - \rho x^0_\alpha x^0_\alpha], \quad (9)$$

describes emission [$\Gamma(1+\bar{n})$ terms], incoherent excitation ($\Gamma\bar{n}$ terms), and pure dephasing (Γ' terms), from the cavity and phonon baths. Note that, importantly, we do not make any secular approximations, though we neglect counter-rotating wave terms that oscillate at $\pm(\omega+\omega')$. The dressed-state operators, solved in a basis of energy eigenstates with respect to H_s, are defined through

$$x^+_\alpha(\omega) = \sum_{j,k>j} \langle j|(O_\alpha)|k\rangle |j\rangle\langle k|$$

$$x^0_\alpha = \sum_j \langle j|(O_\alpha)|j\rangle |j\rangle\langle j|, \quad (10)$$

where $\omega = \omega_k - \omega_j > 0$, $x^- = (x^+)^\dagger$, with $O_c = a + a^\dagger$ and $O_m = b + b^\dagger$.

We have assumed Ohmic bath functions for both cavity and phonon baths [$J_\alpha(\omega) = \Gamma_\alpha \omega/2\pi\omega_\alpha$], and the decay rates are then defined from $\Gamma_\alpha(\omega) = \gamma_\alpha \omega/\omega_\alpha$, and $\Gamma'_\alpha(T) = \gamma_\alpha T/\omega_\alpha$ (bath-induced pure dephasing); the vibrational pure dephasing term becomes especially important at elevated temperatures.

For the TLS pure dephasing term $\mathcal{L}^\phi_G \rho$ (with relevant operator x^0_x and $O_x = \sigma^+\sigma^-$), we use a common spectral function for molecules [19], $J_\phi(\omega) = \eta\omega e^{-\omega^2/\omega^2_{\text{cut}}}$, where $\omega_{\text{cut}} = 160$ meV is the cutoff frequency and η is the coupling strength, which we define from $\gamma_\phi = \Gamma_\phi(0) = 10$ meV at room temperature, and we assume scales linearly with temperature. We can also define the pure dephasing rates explicitly, including $n_x(\omega)$ (upwards transition) and $1+\bar{n}_x(\omega)$ (downward transition):

$$\Gamma^\downarrow_\phi(\omega) = 2\pi J_\phi(\omega)[1+\bar{n}_x(\omega)], \quad \omega \geqslant 0,$$

$$\Gamma^\uparrow_\phi(\omega) = 2\pi J_\phi(-\omega)\bar{n}_x(-\omega), \quad \omega < 0. \quad (11)$$

Finally, in the interaction picture at the laser frequency ω_L, we also add in a coherent cavity pump term, $H_{\text{pump}} = \Omega(a + a^\dagger)$, where Ω is the continuous wave (CW) Rabi frequency. This term also transforms to the dressed-state basis, so that

$$H_{\text{pump}} \rightarrow \Omega(x^+_c + x^-_c), \quad (12)$$

which is included after diagonalizing the density matrix from the solution of H_s. We note that while previous studies with the GME have focused on the quantum Rabi model and optomechanical interactions [39] separately; here, we have a combined interaction with three system operators, and we have also explicitly accounted for a TLS pure dephasing bath as well as a coherent pump field for the cavity mode. This approach also enables us to have clear insights into the underlying dressed resonances.
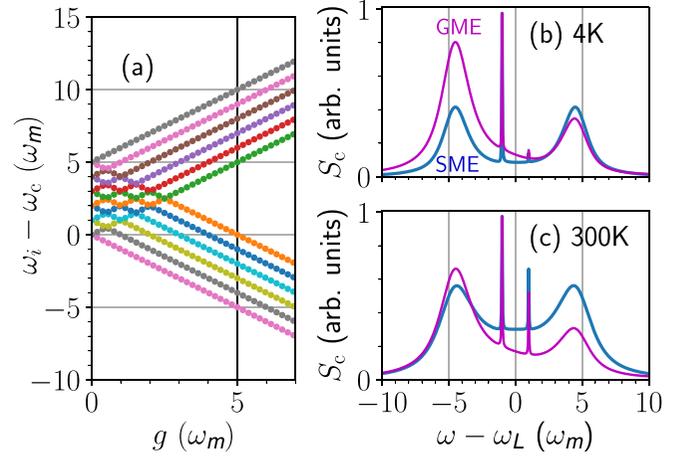
FIG. 2. (a) Eigenfrequencies of the system Hamiltonian [Eq. (5)] for the $n = 1$ photon manifold as a function of g with $d_0 = 0.2$. (b) Cavity emitted spectra with a coherent drive ($\omega_L = \omega_x = \omega_c$) at $g = 5\omega_m$ and 4 K, showing the SME solution [Eq. (6), blue solid curve] and GME solution [Eq. (8), magenta solid curve]. (c) Cavity emitted spectra at 300 K.

Numerically, we obtain an appropriately large number of energy states from a basis of n photons, m phonons, and the TLS, and we truncate to the lowest N levels in the dressed-state basis and check that this truncation is numerically conserved for each problem studied below. Simulations are performed using QUTIP [40].

III. RESULTS

A. System parameters

For the MNP of interest, we consider cavity mode parameters representative of metal dimers with a small gap, ranging from 0.5 to 2 nm to create a pronounced field hot spot [18]. The dissipative open-cavity modes can be quantitatively described using quasinormal modes (QNMs) [41–43], which are solutions to the source-free Maxwell equations with open boundary conditions. Even for the smallest gap, the entire response is very well explained with a single QNM [18]. The QNM complex eigenfrequencies are defined from $\tilde{\omega}_c = \omega_c - i\gamma_c$, where $\kappa = 2\gamma_c$, $Q = \omega_c/\kappa$ and the effective mode volume is obtained from the normalized QNM spatial profile at the dimer gap center [41]. For resonant SERS, we choose values of $d_0 = 0.2$–1 [20,44], where $d_0 = 1$ corresponds to $g_{\text{om}} = \omega_m$. For the molecular vibrational mode, we consider a smaller-frequency oscillation at $\hbar\omega_m = 20$ meV as well as a higher-frequency oscillation at $\hbar\omega_m = 160$ meV, with $\gamma_m = 0.8$ meV. For the cavity mode, we use $\kappa = 100$ meV and $\omega_c = \omega_x = 1.7$ eV.

B. Strong cavity-exciton coupling and ultrastrong vibrational coupling with $g > \omega_m$

We first consider a regime where $\omega_m = 20$ meV and $g = \omega_m = \kappa$, with $d_0 = 0.2$.

Figure 2(a) shows the eigenenergies without dissipation as a function of g, for the first six phonon levels in the $n = 1$ photon subspace. At $g = 5\omega_m$, the $k = 1$ lower polariton shifts

down to $-5\omega_m$, with the phonon states split by exactly one phonon frequency; a similar trend happens at the upper polariton states. In the $n = 0$ photon subspace, we simply obtain constant energy levels split by ω_m. Since photon transitions can take place from any of these excited phonon states, in general the splitting will always be less than ω_m, even when $\kappa \ll g$.

To access these energy states in the presence of resonant Raman scattering, we calculate the emitted spectrum in the presence of the CW field $\Omega = 0.25g$. We calculate the cavity emitted spectrum of the hybrid system from $S_c(\omega) \equiv \text{Re}\{\int_0^\infty dt \, e^{i(\omega_L - \omega)t}[\langle x_c^-(t)x_c^+(0)\rangle_{ss} - \langle x_c^-\rangle_{ss}\langle x_c^+\rangle_{ss}]\}$, where the expectation values are taken over the system steady state.

Figure 2(b) displays the results at a temperature of 4 K, showing the first Stokes and anti-Stokes sidebands as $\pm\omega_m$, and polariton peaks around $\pm 4.5\omega_m$; these resonances are not increased with smaller κ and are due to the collective summation of the phonon-dressed states contributing to the emission linewidth. The sharp Raman spectral features stem from long-lived Raman oscillations that damp as the bath-modified phonon decay rates, and these damp further with increasing drive strengths. Interestingly, we also see a pronounced asymmetry in the GME calculations [45], which for this example is mainly coming from the spectral properties of the TLS dephasing bath. This shows that even though the zero-phonon line has negligible dephasing, the properties of the bath at the dressed resonances have a substantial influence on the oscillator strengths. The bath-induced resonances cause downward transitions between the upper polariton and lower polariton states, while the transitions from the lower to higher states are negligible at low temperatures.

Figure 2(c) shows the results at $T = 300$ K, which confirms that these effects survive at elevated temperatures, and the bath-induced asymmetry is still visible but less pronounced in the GME, since now there is a larger probability also for bath-induced upwards transitions between the polariton states; the anti-Stokes Raman transition is also much more visible.

A spectral asymmetry has been shown also using a SME approach with effective Lindblad operators in a single exciton subspace [21], though the general spectra trends as a function of temperature are quite different. For example, we obtain clear Stokes and anti-Stokes signals even at 300 K and qualitatively different spectra at low temperatures. Apart from requiring multiple input states for our GME model, it is important to note that for a bath in thermal equilibrium, one must satisfy detailed balance [38,46], $\Gamma_\phi^\uparrow(\omega) = e^{\omega/T}\Gamma_\phi^\downarrow(\omega)$. Outside the regime of resonant Raman scattering and nonlinear driving, the role of phonon-induced asymmetry in vacuum Rabi splitting has been shown to be important in various cavity-QED systems, including molecules [19,30] and electron-phonon scattering in quantum dot systems [32–34,47,48].

C. Strong cavity coupling and ultrastrong vibrational coupling with $\omega_m > g$

We next explore polariton-dressed Raman transitions and consider a regime where $\omega_m = 160$ meV and $g = 2/3\,\omega_m$, for
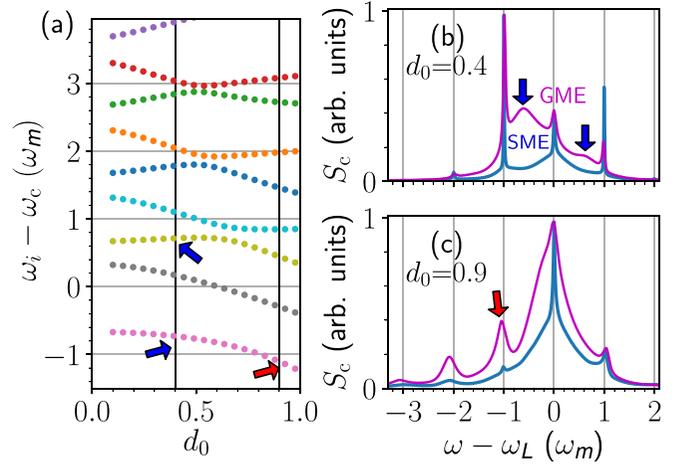
FIG. 3. (a) Eigenfrequencies of the system Hamiltonian [Eq. (5)] for the $n = 1$ photon manifold as a function of d_0 with $g = 80$ meV and $\omega_m = 120$ meV. (b) Cavity emitted spectra with a coherent drive at $d_0 = 0.4$, at $T = 4$ K, showing the SME [Eq. (6), blue solid curve] and GME solution [Eq. (8), magenta solid curve]. (c) Cavity emitted spectra at $d_0 = 0.9$. Arrows show some characteristic resonances.

several different values of d_0, and all other parameters remain the same as before.

Figure 3(a) shows the system eigenenergies as a function of d_0, which are much richer than the previous example. The first and third levels correspond to the polariton states with $k = 0$ (zero phonons), which can be dressed by an increasing d_0, and the third level anticrosses with the $k = 2$ lower polariton state around $d_0 = 0.6$. The second resonance (from the bottom) corresponds to the $k = 1$ lower polariton state, which decreases as a function of d_0.

Figure 3(b) shows the cavity emitted spectra at $d_0 = 0.4$, and we label some of the zero-phonon polariton states with arrows; these resonances clearly show up before the first Raman sidebands and interestingly are not visible in the SME simulations; they also become more pronounced for smaller κ.

Figure 3(c) shows the cavity emitted spectra at $d_0 = 0.9$, where we see that the first Stokes resonance is shifted down from $-\omega_m$; there is also rich structure at the red side of the center frequency, which originates from the second lowest resonance in Fig. 3(a). These results are qualitatively similar at elevated temperatures, with the SME drastically failing throughout the entire frequency range. In this example, asymmetries form the TLS pure dephasing bath are negligible but are mainly caused by the larger d_0 causing phonon modifications to the vibrational and cavity emission and excitation dissipator terms in the GME.

Finally, we study how the dressed resonances influence the mean populations versus laser detuning, which can be accessed experimentally from the photoluminescence spectra [31]. The steady-state populations of the cavity mode, vibrational mode, and TLS are obtained from $n_i = \langle x_i^- x_i^+\rangle$. Figure 4 shows the eigenenergies at $d_0 = 0.6$, using the same parameters as in Fig. 3. Figure 4(b) displays the mean populations as a function of laser-exciton detuning, where the first phonon resonance near zero detuning is clearly showing
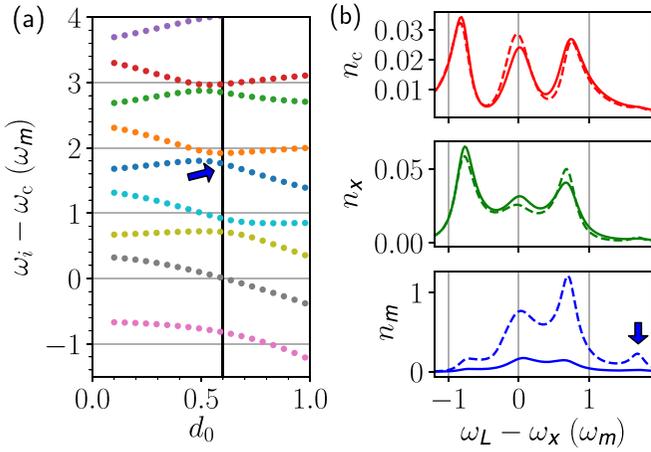
FIG. 4. (a) As in Fig. 3(a), but showing resonances at $d_0 = 0.6$. (b) Steady-state populations as a function of laser detuning for the cavity, exciton, and phonon. The dashed (solid) curves show the SME (GME) solutions.

up, and we also see the fifth resonance, which is the $k = 1$ upper polariton state (marked by a blue arrow). We note that the phonon populations are completely overestimated with the SME as the phonon displacement acts to increase the phonon damping in the vibrational USC regime. In addition, we see modified spectral asymmetries [45] in both the cavity and exciton profiles.

IV. CONCLUSIONS

In summary, we have presented a GME approach to describe the regime of cavity-QED strong coupling under vibrational USC, demonstrating several rich regimes of single molecule optomechanics, in regimes where the SME significantly fails. We demonstrated how phonons *dress* the polariton states of strong cavity-exciton coupling, which also leads to pronounced spectral asymmetries from TLS pure dephasing and other bath-induced resonances, even at low temperatures. With increased exciton-phonon coupling, we also explored a regime where both cavity coupling and phonon coupling act in concert to produce new polariton states that appear below the Raman sidebands, and where fundamentally new resonances appear, which are visible in the cavity emitted and photoluminescence spectra. In all cases, we showed explicitly that the SME significantly fails. All our predictions use system parameters similar to recent experiments and thus should be within experimental reach.

APPENDIX: CONNECTION BETWEEN OFF-RESONANT SERS AND RESONANT SERS FROM A POLARONIC PICTURE

To make the connection between off-resonant SERS and resonant SERS clear, it is useful to consider the system Hamiltonians in a polaronic picture, which has certain advantages in handling nonperturbative phonon (vibrational) coupling. Below we discuss how these two forms relate to each other, and when they are drastically different in general. Similar analogies have been pointed out in Refs. [18] and [20], but without formal definitions of the polaron transforms.

Specifically, the resonant SERS scheme we study in the main text is substantially different from the off-resonant SERS scheme. The latter (off-resonant form) is related to the usual optomechanical Hamiltonian, and the former (on-resonant form) fully recovers the physics of the Jaynes-Cummings model with phonon interactions turned off (and includes three system operators, not two). Our phonon interactions are also included without any approximations, as is required for studies in the vibronic ultrastrong coupling regime, requiring a full nonlinear and nonperturbative treatment, as well as a careful consideration for system-bath interactions.

1. Off resonant Raman interactions

For *off-resonant* Raman interactions (usual SERS form), we consider the standard optomechanical interaction without any form of linearization [25] and neglect optical pumping,

$$H_s^{\text{off−res}} = \omega_c a^\dagger a + \omega_m b^\dagger b + g_{\text{om}} a^\dagger a(b^\dagger + b), \quad \text{(A1)}$$

where cavity operator terms aa and $a^\dagger a^\dagger$ (dynamical Casimir effects) can be safely ignored here, as $\omega_c \gg \omega_m$. The optomechanical coupling factor is given by [14]

$$g_{\text{om}} = (R_m/2\omega_m)^{-1/2}\frac{\omega_c}{\epsilon_0 V_c}, \quad \text{(A2)}$$

with R_m being the Raman activity [49] associated with the vibrational mode under study and V_c being the effective mode volume of the cavity mode [14]. Note that the same concept has also been extended to arbitrary bath media [16] (e.g., not just at the level of simple coupled mode theory).

Since the eigenstates are tensor products of fixed number states with displaced harmonic-oscillator eigenstates, the polaron transform here is just an $a^\dagger a$-dependent displacement of the mechanical resonator: $\hat{S} = d a^\dagger a(b^\dagger - b)$. The polaron transformed system Hamiltonian for *off-resonant SERS*, $\tilde{H}_s^{\text{off−res}} = e^{\hat{S}} H_s^{\text{off−res}} e^{-\hat{S}}$, is then

$$\tilde{H}_s^{\text{off−res}} = (\omega_c - \Delta_P)a^\dagger a + \omega_m b^\dagger b - \Delta_P a^\dagger a^\dagger aa, \quad \text{(A3)}$$

where $a \to a\hat{X}$, and the displacement operator is $\hat{X} = \exp[d(b - b^\dagger)]$. In the polaron frame, the effective cavity resonance is shifted down by $\Delta_P = g_{\text{om}}^2/\omega_m = d^2\omega_m$ (well-known polaron shift), as also shown from the eigenvalues of the optomechanical coupling problem (discussed in Sec. II of this paper). The Kerr-like term (four operators) causes a nonlinear dependence on photon number (photon-photon interaction), and *if* this term can be neglected, then one can write

$$\tilde{H}_s^{\text{off}-\text{res}} \approx (\omega_c - \Delta_P)a^\dagger a + \omega_m b^\dagger b, \qquad (A4)$$

which is clearly in a much simpler form. Note that the nonlinearities in this optomechanical coupling term are not the same as a Fermionic system, since all operators here are bosons.

2. Resonant Raman interactions

For *resonant Raman interactions* (see Fig. 1), the system Hamiltonian is now

$$H_s^{\text{on}-\text{res}} = \omega_c a^\dagger a + \omega_m bb^\dagger + \omega_x \sigma^+\sigma^- +$$
$$+ d_0\omega_m \sigma^+\sigma^-(b^\dagger + b) + g(\sigma^+ a + a^\dagger \sigma^-), \quad (A5)$$

where the latter term is the Jaynes-Cummings term and, as noted in the main text, we assume $g \ll \omega_c$, so as to neglect USC effects related to the TLS-cavity coupling. Note that we are now dealing with three system operators, two bosonic and one Fermionic. The polaron transformed system Hamiltonian, for resonant SERS, now using $\hat{S} = d_0\sigma^+\sigma^-(b^\dagger - b)$ and $\hat{X} = \exp[d_0(b - b^\dagger)]$, is

$$\tilde{H}_s^{\text{on}-\text{res}} = \omega_c a^\dagger a + \omega_m bb^\dagger + (\omega_x - \Delta_P)\sigma^+\sigma^-$$
$$+ g(\sigma^+ a\hat{X} + a^\dagger \hat{X}^\dagger \sigma^-). \qquad (A6)$$

The equivalence between the off-resonant and resonant SERS can be made with a harmonic-oscillator approximation for the TLS in a bad-cavity limit. Specifically, the resonant SERS polaron transformed Hamiltonian then becomes identical in form to the off-resonance case, apart from the Kerr-like term (which vanishes for Fermions), and one simply replaces $a, a^\dagger$ with σ^-, σ^+ and identifies $d = d_0$. When Fermionic behavior becomes important in the two-state system (e.g., Mollow physics, strong coupling between the cavity mode and two-level system), then clearly one must use the Pauli operators, and the off-resonant SERS Hamiltonian is no longer appropriate. Indeed, in a good-cavity regime, and with nonlinear resonant excitation and cavity-QED interactions, the systems are vastly different.

[1] C. V. Raman and K. S. Krishnan, A new type of secondary radiation, Nature (London) **121**, 501 (1928).

[2] G.-Y. Chen, N. Lambert, C.-H. Chou, Y.-N. Chen, and F. Nori, Surface plasmons in a metal nanowire coupled to colloidal quantum dots: Scattering properties and quantum entanglement, Phys. Rev. B **84**, 045310 (2011).

[3] M. S. Tame, K. R. McEnery, Ş. K. Özdemir, J. Lee, S. A. Maier, and M. S. Kim, Quantum plasmonics, Nat. Phys. **9**, 329 (2013).

[4] A. Regler, K. Schraml, A. A. Lyamkina, M. Spiegl, K. Müller, J. Vuckovic, J. J. Finley, and M. Kaniber, Emission redistribution from a quantum dot-bowtie nanoantenna, J. Nanophotonics **10**, 033509 (2016).

[5] T. Cai, S. Dutta, S. Aghaeimeibodi, Z. Yang, S. Nah, J. T. Fourkas, and E. Waks, Coupling emission from single localized defects in two-dimensional semiconductor to surface plasmon polaritons, Nano Lett. **17**, 6564 (2017).

[6] R. Chikkaraddy, B. de Nijs, F. Benz, S. J. Barrow, O. A. Scherman, E. Rosta, A. Demetriadou, P. Fox, O. Hess, and J. J. Baumberg, Single-molecule strong coupling at room temperature in plasmonic nanocavities, Nature (London) **535**, 127 (2016).

[7] A. Ridolfo, O. Di Stefano, N. Fina, R. Saija, and S. Savasta, Quantum Plasmonics with Quantum Dot-Metal Nanoparticle Molecules: Influence of the Fano Effect on Photon Statistics, Phys. Rev. Lett. **105**, 263601 (2010).

[8] R.-C. Ge, C. V. Vlack, P. Yao, J. F. Young, and S. Hughes, Accessing quantum nanoplasmonics in a hybrid quantum dot–metal nanosystem: Mollow triplet of a quantum dot near a metal nanoparticle, Phys. Rev. B **87**, 205425 (2013).

[9] C. Belacel, B. Habert, F. Bigourdan, F. Marquier, J.-P. Hugonin, S. M. de Vasconcellos, X. Lafosse, L. Coolen, C. Schwob, C. Javaux, B. Dubertret, J.-J. Greffet, P. Senellart, and A. Maitre,

Controlling spontaneous emission with plasmonic optical patch antennas, Nano Lett. **13**, 1516 (2013).

[10] G. M. Akselrod, C. Argyropoulos, T. B. Hoang, C. Ciracì, C. Fang, J. Huang, D. R. Smith, and M. H. Mikkelsen, Probing the mechanisms of large Purcell enhancement in plasmonic nanoantennas, Nat. Photonics **8**, 835 (2014).

[11] R.-C. Ge and S. Hughes, Quantum dynamics of two quantum dots coupled through localized plasmons: An intuitive and accurate quantum optics approach using quasinormal modes, Phys. Rev. B **92**, 205420 (2015).

[12] P.-C. Kuo, N. Lambert, A. Miranowicz, H.-B. Chen, G.-Y. Chen, Y.-N. Chen, and F. Nori, Collectively induced exceptional points of quantum emitters coupled to nanoparticle surface plasmons, Phys. Rev. A **101**, 013814 (2020).

[13] P. Rabl, Photon Blockade Effect in Optomechanical Systems, Phys. Rev. Lett. **107**, 063601 (2011).

[14] P. Roelli, C. Galland, N. Piro, and T. J. Kippenberg, Molecular cavity optomechanics as a theory of plasmon-enhanced Raman scattering, Nat. Nanotechnol. **11**, 164 (2015).

[15] M. K. Schmidt, R. Esteban, A. González-Tudela, G. Giedke, and J. Aizpurua, Quantum mechanical description of Raman scattering from molecules in plasmonic cavities, ACS Nano **10**, 6291 (2016).

[16] M. Kamandar Dezfouli and S. Hughes, Quantum optics model of surface-enhanced Raman spectroscopy for arbitrarily shaped plasmonic resonators, ACS Photonics **4**, 1245 (2017).

[17] A. Lombardi, M. K. Schmidt, L. Weller, W. M. Deacon, F. Benz, B. de Nijs, J. Aizpurua, and J. J. Baumberg, Pulsed Molecular Optomechanics in Plasmonic Nanocavities: From Nonlinear Vibrational Instabilities to Bond-Breaking, Phys. Rev. X **8**, 011016 (2018).

[18] M. K. Dezfouli, R. Gordon, and S. Hughes, Molecular optomechanics in the anharmonic cavity-QED regime using hybrid metal–dielectric cavity modes, ACS Photonics **6**, 1400 (2019).

[19] J. del Pino, J. Feist, and F. J. Garcia-Vidal, Signatures of vibrational strong coupling in Raman scattering, J. Phys. Chem. C **119**, 29132 (2015).

[20] T. Neuman, R. Esteban, G. Giedke, M. K. Schmidt, and J. Aizpurua, Quantum description of surface-enhanced resonant Raman scattering within a hybrid-optomechanical model, Phys. Rev. A **100**, 043422 (2019).

[21] T. Neuman, J. Aizpurua, and R. Esteban, Quantum theory of surface-enhanced resonant Raman scattering (SERRS) of molecules in strongly coupled plasmon–exciton systems, Nanophotonics **9**, 295 (2020).

[22] J. Calvo, D. Zueco, and L. Martin-Moreno, Ultrastrong coupling effects in molecular cavity QED, Nanophotonics **9**, 277 (2020).

[23] A. F. Kockum, A. Miranowicz, S. D. Liberato, S. Savasta, and F. Nori, Ultrastrong coupling between light and matter, Nat. Rev. Phys. **1**, 19 (2019).

[24] P. Forn-Díaz, L. Lamata, E. Rico, J. Kono, and E. Solano, Ultrastrong coupling regimes of light-matter interaction, Rev. Mod. Phys. **91**, 025005 (2019).

[25] M. Aspelmeyer, T. J. Kippenberg, and F. Marquardt, Cavity optomechanics, Rev. Mod. Phys. **86**, 1391 (2014).

[26] G. S. Agarwal, *Quantum Optics* (Cambridge University Press, Cambridge, 2012).

[27] K. Huang and A. Rhys, Theory of light absorption and non-radiative transitions in *F*-centres, Proc. R. Soc. London, Ser. A **204**, 406 (1950).

[28] R. Kubo and Y. Toyozawa, Application of the method of generating function to radiative and non-radiative transitions of a trapped electron in a crystal, Prog. Theor. Phys. **13**, 160 (1955).

[29] G. D. Mahan, *Many-Particle Physics* (Springer, New York, 2000).

[30] T. Neuman and J. Aizpurua, Origin of the asymmetric light emission from molecular exciton–polaritons, Optica **5**, 1247 (2018).

[31] S. Weiler, A. Ulhaq, S. M. Ulrich, D. Richter, M. Jetter, P. Michler, C. Roy, and S. Hughes, Phonon-assisted incoherent excitation of a quantum dot and its emission properties, Phys. Rev. B **86**, 241304(R) (2012).

[32] K. Roy-Choudhury and S. Hughes, Quantum theory of the emission spectrum from quantum dots coupled to structured photonic reservoirs and acoustic phonons, Phys. Rev. B **92**, 205406 (2015).

[33] P. Kaer and J. Mørk, Decoherence in semiconductor cavity QED systems due to phonon couplings, Phys. Rev. B **90**, 035312 (2014).

[34] I. Wilson-Rae and A. Imamoğlu, Quantum dot cavity-QED in the presence of strong electron-phonon interactions, Phys. Rev. B **65**, 235311 (2002).

[35] H.-P. Breuer and F. Petruccione, *The Theory of Open Quantum Systems* (Oxford University Press, Oxford, 2007).

[36] H. J. Carmichael, *Statistical Methods in Quantum Optics I* (Springer, New York, 2002).

[37] H. J. Carmichael and D. F. Walls, Master equation for strongly interacting systems, J. Phys. A: Math., Nucl. Gen. **6**, 1552 (1973).

[38] F. Beaudoin, J. M. Gambetta, and A. Blais, Dissipation and ultrastrong coupling in circuit QED, Phys. Rev. A **84**, 043832 (2011).

[39] A. Settineri, V. Macrí, A. Ridolfo, O. D. Stefano, A. F. Kockum, F. Nori, and S. Savasta, Dissipation and thermal noise in hybrid quantum systems in the ultrastrong-coupling regime, Phys. Rev. A **98**, 053834 (2018).

[40] J. R. Johansson, P. D. Nation, and F. Nori, Qutip: An open-source Python framework for the dynamics of open quantum systems, Comput. Phys. Commun. **183**, 1760 (2012).

[41] P. T. Kristensen and S. Hughes, Modes and mode volumes of leaky optical cavities and plasmonic nanoresonators, ACS Photonics **1**, 2 (2014).

[42] M. Kamandar Dezfouli, R. Gordon, and S. Hughes, Modal theory of modified spontaneous emission of a quantum emitter in a hybrid plasmonic photonic-crystal cavity system, Phys. Rev. A **95**, 013846 (2017).

[43] P. Lalanne, W. Yan, K. Vynck, C. Sauvan, and J.-P. Hugonin, Light interaction with photonic and plasmonic resonances, Laser Photonics Rev. **12**, 1700113 (2018).

[44] R. S. Sánchez-Carrera, M. C. R. Delgado, C. C. Ferrón, R. M. Osuna, V. Hernández, J. T. L. Navarrete, and A. Aspuru-Guzik, Optical absorption and emission properties of end-capped oligothienoacenes: A joint theoretical and experimental study, Org. Electron. **11**, 1701 (2010).

[45] X. Cao, J. Q. You, H. Zheng, and F. Nori, A qubit strongly coupled to a resonant cavity: asymmetry of the spontaneous emission spectrum beyond the rotating wave approximation, New J. Phys. **13**, 073002 (2011).

[46] A. A. Clerk, M. H. Devoret, S. M. Girvin, F. Marquardt, and R. J. Schoelkopf, Introduction to quantum noise, measurement, and amplification, Rev. Mod. Phys. **82**, 1155 (2010).

[47] F. Milde, A. Knorr, and S. Hughes, Role of electron-phonon scattering on the vacuum Rabi splitting of a single-quantum dot and a photonic crystal nanocavity, Phys. Rev. B **78**, 035330 (2008).

[48] E. V. Denning, M. Bundgaard-Nielsen, and J. Mørk, Optical signatures of electron-phonon decoupling due to strong light-matter interactions, Phys. Rev. B **102**, 235303 (2020).

[49] Note that the Raman activity is related to the elements of the Raman tensor but they have different units.